

# WP1066 exhibits antitumor efficacy in nasal-type natural killer/T-cell lymphoma cells through downregulation of the STAT3 signaling pathway

LINGYUN GENG, XINYU LI, XIANGXIANG ZHOU, XIAOSHENG FANG, DAI YUAN and XIN WANG

Department of Hematology, Shandong Provincial Hospital Affiliated to Shandong University, Jinan, Shandong 250021, P.R. China

Received March 1, 2016; Accepted July 11, 2016

DOI: 10.3892/or.2016.5091

**Abstract.** Nasal-type natural killer/T-cell lymphoma (nasal NKTCL) is an aggressive hematological neoplasm with poor prognosis, and its incidence is higher in Asia than in Western countries. Increasing evidence suggests that aberrant activation of signal transducers and activators of transcription 3 (STAT3) is related to numerous malignancies. However, the involvement of STAT3 in the pathogenesis of nasal NKTCL is poorly understood. In this study, immunohistochemistry (IHC) showed that 21/28 (75.0%) nasal NKTCL tissues harbored constitutively expression of phospho-STAT3 (p-STAT3) which was positively correlated with the Ki-67 levels ( $P < 0.05$ ). Immunofluorescence (IF) also detected p-STAT3 expression in SNK6 cells (NKTCL cell line). Furthermore, WP1066 (a novel selective STAT3 inhibitor) was able to inhibit proliferation and induce apoptosis of SNK6 cells. Moreover, western blot analysis and RT-PCR demonstrated that WP1066 downregulated the protein and mRNA expressions of the pro-survival molecules (including c-Myc, cyclin D1, and Bcl-2) in SNK6 cells. These results suggested that STAT3 activation represents a potential target in nasal NKTCL. WP1066 may be a promising agent in antitumor therapy against nasal NKTCL.

## Introduction

Nasal-type natural killer/T-cell lymphoma (nasal NKTCL), is a rare subtype of non-Hodgkin's lymphoma (NHL) derived from natural killer (NK) cells and, more rarely, T cells closely correlate with Epstein-Barr virus (EBV) infection (1).

Its frequency among all lymphoma is ~3-10% in East Asia, but <1% in Western countries (2). Even though 2/3 of nasal NKTCL patients present with localized lesions, the prognosis of nasal NKTCL remains dismal because of its aggressive course and resistance to conventional chemotherapy (3,4). Genetic variants, cellular immune deficiency, and EBV infection have been implicated in the molecular pathogenesis of nasal NKTCL (5). The exact etiology is still ambiguous, and therefore the best first-line therapeutic strategies have not been established (6).

Signal transducers and activators of transcription 3 (STAT3), a major component of the STAT family, has been established to play important roles in the development and progression of many human malignancies, such as glioma, pancreatic cancer, prostate cancer, anaplastic large cell lymphoma, and T-cell large granular lymphocyte leukemia (7-10). Phosphorylation of STAT3 triggers its dimerization and nuclear transport, where it promotes the transcription of genes that stimulate tumor growth. Thus phospho-STAT3 (p-STAT3) was used as a measurement of STAT activation. Briefly, multiple pathways unify and use STAT3 as a central molecular hub (11-14). Inappropriately activated STAT3, located at the converging point of various signaling networks, ultimately activated multiple downstream genes that facilitate tumor invasion, metastasis, and angiogenesis, but suppressed host immune surveillance (15-18). In light of this role, inhibitors of the STAT3 pathway are attractive therapeutic targets for cancer. WP1066 represents a novel promising STAT3 inhibitor in antitumor therapy (19,20). However, the involvement of STAT3 activation in the development of nasal NKTCL is still poorly understood.

In the present study we detected the STAT3 activity in nasal NKTCL tissues and cell line, and investigated the inhibitory effect and the underlying mechanisms of WP1066 (small molecule STAT3 inhibitor) in the nasal NKTCL cells.

## Materials and methods

**Cell line and culture.** The human NKTCL SNK6 cell line was cultured in RPMI-1640 (Gibco) supplemented with 1% penicillin/streptomycin mixture, 2 mM L-glutamine, 1,000 U/ml interleukin (IL)-2 (Beijing SL Pharmaceutical Co.,

---

*Correspondence to:* Professor Xin Wang, Department of Hematology, Shandong Provincial Hospital Affiliated to Shandong University, 324 Jingwu Road, Jinan, Shandong 250021, P.R. China  
E-mail: xinw007@126.com

**Key words:** nasal-type natural killer/T-cell lymphoma, signal transducers and activators of transcription 3 inhibitor, apoptosis, targeted therapy

Ltd., Beijing, China), and 10% human AB serum provided by the Blood Center of Shandong Province (Jinan, China) in 5% CO<sub>2</sub> at 37°C.

**Patients and tissues.** The paraffin-embedded tissues from 28 cases of nasal NKTCL (19 males and 9 females; age range 24-72 years, median 47.5 years) were collected from Shandong Provincial Hospital affiliated to Shandong University prior to therapeutic intervention in this study. All patients were diagnosed according to the WHO criteria between January 2009 and June 2015. Reactive hyperplasia of lymph node (RHLN) served as control. This study was approved by the Medical Ethics Committee of Shandong Provincial Hospital affiliated to Shandong University. All human samples were obtained after informed consents had been given, according to the Declaration of Helsinki.

**Reagents.** STAT3 inhibitor WP1066, purchased from Selleck Chemicals (Boston, MA, USA), was dissolved in DMSO to make the stock solution. Stock solution was finally diluted into cell culture medium to make the final working concentrations.

**Immunohistochemistry (IHC).** IHC of patients' paraffin-embedded tissue sections was performed using primary rabbit antibodies for p-STAT3 (Tyr705) (Cell Signaling Technology, Danvers, MA, USA). Briefly, formalin-fixed, paraffin-embedded tissue sections of 4 mM thickness were deparaffinized and hydrated. High-pressure antigen retrieval was performed in 0.01 M sodium citrate (pH 6.0). Endogenous peroxidase was blocked with 3% H<sub>2</sub>O<sub>2</sub> in methanol for 15 min at room temperature, followed by incubation with normal serum to block non-specific staining. Primary rabbit antibodies were diluted as p-STAT3 (Tyr705) (1:400) applied to incubate the sections overnight in a humidified chamber at 4°C; then the second antibody from SP reagent kit (Zhongshan Goldenbridge Biotechnology Co., Beijing, China) was used to incubate the sections for 1 h at room temperature. After washing, the tissue sections were treated with biotinylated anti-rabbit secondary antibody, followed by further incubation with streptavidin-horseradish peroxidase complex. After staining with 3,3'-diaminobenzidine kit (DAB; Zhongshan Goldenbridge Biotechnology Co.), the sections were counterstained with hematoxylin and mounted. Immunohistochemical staining was assessed in a series of randomly selected five high-power fields, which were believed to be representative of the average in tumors at x400 magnification, by two independent observers who were blinded to all clinical data. Tumors displaying staining in ≥30% of the cells were categorized as positive cases, whereas, tumors displaying staining <30% of the cells were categorized as negative cases.

**Immunofluorescence (IF).** SNK6 cells were cultured for 24 h in the presence or absence of 5 μM WP1066. After cytopsin, cells were fixed in acetone and methanol (1:1) for 15 min at room temperature; after three washes in PBS for 10 min each, they were blocked in PBS with 10% donkey serum for 1 h at room temperature. Then the cells were incubated with primary rabbit anti-p-STAT3 (Tyr705) antibody (1:100; Cell Signaling Technology) overnight at 4°C in a humidified chamber. After three washes the following day, cells were incubated with

the secondary antibody Alexa Fluor 568-labeled donkey anti-rabbit IgG antibody (1:500; Invitrogen, Eugene, OR, USA) for 1 h at room temperature in the dark. After washing three times with PBS, 4',6-diamidino-2-phenylindole (DAPI) was used to stain nuclei followed by analysis using confocal microscopy (LSM 780; Carl Zeiss).

**Assessment of cell proliferation.** The influence of WP1066 on viability of SNK6 cells was assessed by carrying out triplicate assays with the Cell Counting kit-8 (CCK-8; Dojindo, Kumamoto, Japan). SNK6 cells (5,000 cells/100 μl/well, respectively) were seeded into 96-well plates at 37°C with 5% CO<sub>2</sub> and incubated with WP1066 at designated concentrations (0, 0.625, 1.25, 2.5, 5 and 10 μM) for 24 h. Thereafter, the cells were incubated with 10 μl of CCK-8 for 4 h according to the manufacturer's instructions. The absorbance at 450 nm was measured using a SpectraMax M2 Multi-Mode Microplate Reader (Molecular Devices, Sunnyvale, CA, USA). The micrographs of SNK cells after WP1066 incubation were also recorded.

**Analysis of cell apoptosis.** Effects of WP1066 on apoptosis of SNK6 cells were evaluated by Annexin V-phycoerythrin (PE)/7-aminoactinomycin D (7-AAD) assay. Flow cytometric analysis of these cells labeled with Annexin V-PE and 7-AAD was performed according to the manufacturer's instructions (BD Biosciences). Cells with designated treatments were harvested, washed twice with cold PBS and resuspended in 1X binding buffer at a concentration of 1x10<sup>6</sup> cells/ml. This was followed by transferring 100 μl of the solution to a 5 ml tube, to which 5 μl of Annexin V-PE and 5 μl of 7-AAD were added. The tube was gently vortexed and incubated for 15 min at room temperature in the dark. At the end of incubation, 400 μl of 1X binding buffer was added. The rates of cellular apoptosis were acquired immediately on a Navios Flow Cytometer (Beckman Coulter). Viable cells are not stained with Annexin V-PE or 7-AAD. The necrotic cells were Annexin V-PE and 7-AAD-positive, whereas apoptotic cells were Annexin V-PE-positive and 7-AAD-negative.

**Western blot analysis.** Total protein was extracted from SNK6 cells with the treatment. Total protein was extracted using lysis buffer (Shenergy Biocolor, Shanghai, China) and 1% PhosSTOP (Roche, Mannheim, Germany). The protein concentration was determined by the BCA assay (Shenergy Biocolor). Cell lysate was then electrophoresed on 10% SDS-polyacrylamide gels and transferred onto polyvinylidene difluoride (PVDF) membranes. The membranes were blocked with 5% skim-milk in Tris-saline buffer with 0.1% Tween-20, and then incubated with primary antibodies at 4°C overnight. After washing with TBST, secondary antibody conjugated with the horseradish peroxidase (Zhongshan Goldenbridge Biotechnology Co.) was added to the membranes. Proteins were detected using the chemiluminescence detection kit (Millipore, USA). Primary antibodies against p-STAT3 (Tyr705) (1:2,000), STAT3 (1:1,000), c-Myc (1:1,000), cyclin D1 (1:1,000), and Bcl-2 (1:1,000) were purchased from Cell Signaling Technology. The expression level of β-actin was used as the loading control for the western blot analysis. Western blot analysis results were analyzed using

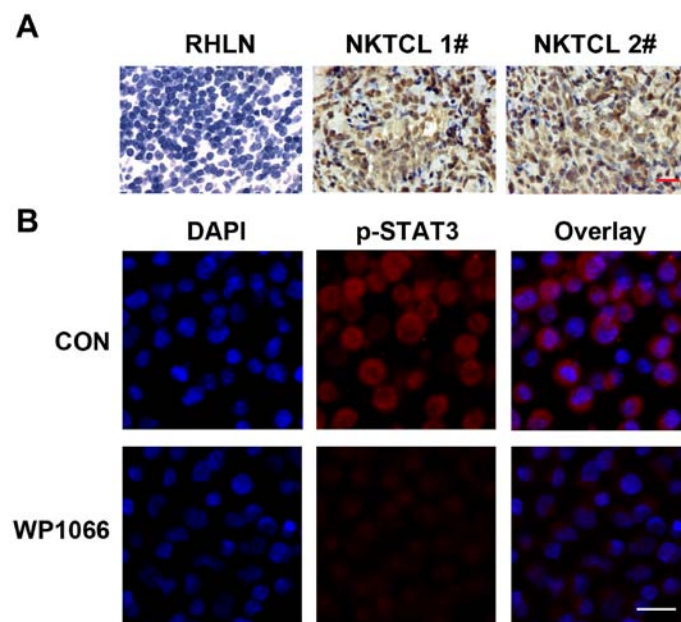


Figure 1. Protein expression of phospho-STAT3 (p-STAT3) in nasal-type natural killer/T-cell lymphoma (nasal NKTCL) tissues and SNK6 cells. (A) Representative images of immunohistochemistry (IHC) showing p-STAT3 expression in tissues from reactive hyperplasia of lymph node (RHLN) and nasal NKTCL patients. Scale bar, 20  $\mu\text{m}$ . (B) Immunofluorescence (IF) analysis revealed that p-STAT3 (red) was expressed in SNK6 cells (upper row). The p-STAT3 staining was downregulated significantly in SNK6 cells after incubation with WP1066 at 2.5  $\mu\text{M}$  for 24 h (lower row). Scale bar, 10  $\mu\text{m}$ .

the LAS 4000 Image software and Multi Gauge version 3.0 software (Fujifilm Life Science, Japan).

**Real-time quantitative polymerase chain reaction (RT-qPCR).** The expression of genes was detected by RT-qPCR analysis. Total RNA was extracted by TRIzol reagent (Takara, Dalian, China) from cells following incubation of WP1066 at different concentrations for 24 h. Then the reverse transcription reaction was conducted by means of Takara reverse transcription reagents (Takara). Amplification reactions were performed using a SYBR Premix Ex Taq II kit (Takara) on a LightCycler 480 real-time PCR system (Roche), using  $\beta$ -actin as an internal reference. The  $2^{-\Delta\Delta\text{Ct}}$  method was used for data analysis with LightCycler 480 Gene Scanning version 1.5 software (Roche). The primers of related genes are provided in Table II.

**Statistical analysis.** Results are expressed as mean  $\pm$  standard error of mean (SEM). One-way analysis of variance (ANOVA) or t-tests were used to test for differences between groups. Fisher's exact probability test was used to analyze the correlation between the immunohistochemical expression of p-STAT3 and the clinicopathological parameters of the 28 nasal NKTCL patients.  $P < 0.05$  was accepted as evidence of significance.

## Results

**Protein expression of p-STAT3 in nasal NKTCL tissues and cell line, and the correlation between p-STAT3 and clinicopathological parameters of nasal NKTCL patients.** We examined the expression of p-STAT3 in tissues from 28 cases of nasal NKTCL by IHC. The positive expression of p-STAT3 was detected in 21/28 (75.0%) cases, when tumor tissues displaying staining in  $\geq 30\%$  of the cells were categorized as

positive cases. The expression of p-STAT3 was detected in both tumor and stromal cells, indicating the involvement of p-STAT3 in the tumor microenvironment (Fig. 1A). However, p-STAT3 staining was too weak to be detected in the control RHLN tissues. Moreover, Fisher's exact probability test showed that the immunohistochemical expression of p-STAT3 was positively correlated with Ki-67 levels (proliferative index) of these tumor tissues. However, no correlation was identified between p-STAT3 expression and the other clinical histopathological parameters (Table I). The expression of p-STAT3 in NKTCL cell line SNK6 was also demonstrated by IF using confocal microscopy (Fig. 1B). The blue color labeled the nucleus staining with DAPI, and red color represented the p-STAT3 expression in SNK6 cells.

**WP1066 inhibits proliferation and induces apoptosis of SNK6 cells.** Cytotoxicity of WP1066 on SNK6 cells was evaluated by morphology and the CCK-8 assay after a 24-h WP1066 treatment at different concentrations (0, 0.625, 1.25, 2.5, 5 and 10  $\mu\text{M}$ ). Morphology observations found that the number of SNK6 cells with WP1066 incubation decreased significantly compared to the control group (Fig. 2A). Simultaneously, CCK-8 analysis confirmed that the viability of the SNK6 cells decreased in a dose-dependent manner after a 24-h WP1066 treatment (Fig. 2B). The half maximal inhibitory concentration ( $\text{IC}_{50}$ ) value of WP1066 in SNK6 cells at 24 h was calculated as  $2.62 \pm 0.28 \mu\text{M}$ . Effect of WP1066 on apoptosis of SNK6 cells was assessed after a 24-h WP1066 treatment at different concentrations. Flow cytometric analysis demonstrated that the percentage of apoptotic cells increased significantly at 24 h following medium- to high-concentration WP1066 treatment compared with the solvent treatment groups (control groups) ( $P < 0.05$ ,  $n=3$ ) (Fig. 3A and B).

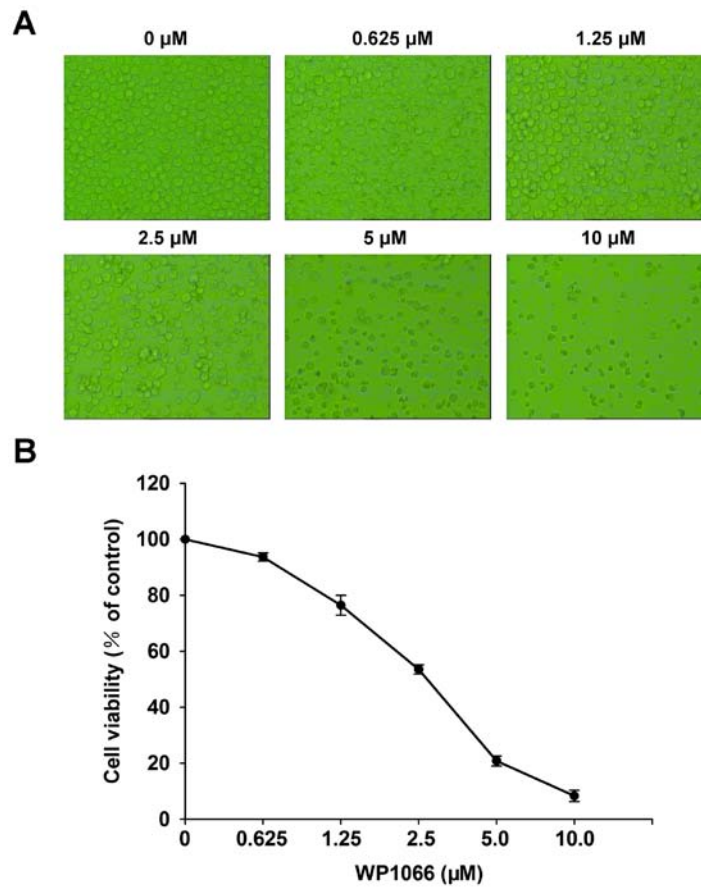


Figure 2. Cytotoxicity of WP1066 on SNK6 cells. (A) Micrograph of SNK6 cells after incubated with different concentrations of WP1066 (0, 0.625, 1.25, 2.5, 5 and 10  $\mu\text{M}$ ) for 24 h. (B) Viability of SNK6 cells was assessed by Cell Counting kit-8 (CCK-8) after a 24-h incubation of WP1066 with the indicated concentrations. The results indicate that WP1066 inhibited the proliferation of SNK6 cells in a dose-dependent manner at 24 h.

Table I. Correlation between p-STAT3 protein expression in nasal NKTCL tissues and the clinicopathological parameters of the 28 nasal NKTCL patients.

	Total no.	p-STAT3		P-value
		Positive	Negative	
Gender				
Male	19	15	4	0.398
Female	9	6	3	
Age (years)				
$\geq 45$	15	12	3	0.412
$< 45$	13	9	4	
EBER				
Positive	20	16	4	0.306
Negative	8	5	3	
Ki-67 (%)				
$\geq 60$	20	18	2	0.009 <sup>a</sup>
$< 60$	8	3	5	

<sup>a</sup>P<0.05, Fisher's exact probability test. p-STAT3, phospho-STAT3; nasal NKTCL, nasal-type natural killer/T-cell lymphoma; EBER, Epstein-Barr virus-encoded small RNA; positive, cells displaying staining accounted for >30%; negative, cells displaying staining accounted for  $\leq 30\%$ .

Table II. PCR primer sequences.

Gene	Primer sequence
c-Myc	5'-GGCTCCTGGCAAAGGTCA-3' 5'-AGTTGTGCTGATGTGTGGAGA-3'
Cyclin D1	5'-CAAATGGAGCTGCTCCTGGTG-3' 5'-CTTCGATCTGCTCCTGGCAGG-3'
Bcl-2	5'-ATGTGTGTGGAGAGCGTCAA-3' 5'-ACAGTTCCACAAAGGCATCC-3'
$\beta$ -actin	5'-TGACGTGGACATCCGCAAAG-3' 5'-CTGGAAGGTGGACAGCGAGG-3'

*Influence of WP1066 on protein expression of p-STAT3 and downstream molecules in SNK6 cells.* Western blot analysis exhibited the decrease of protein expression for p-STAT3 in SNK6 cells after a 24-h treatment of WP1066 in a dose-dependent manner (Fig. 4A and B). Concomitantly, there was a significant reduction in the protein expression of c-Myc, cyclin D1, and Bcl-2 after WP1066 treatment from moderate to high concentration in SNK6 cells (Fig. 4C). The inhibitory effect of WP1066 on phosphorylation of STAT3 in SNK6 cells was also confirmed by IF analysis. WP1066 treatment brought about a significant downregulation of p-STAT3

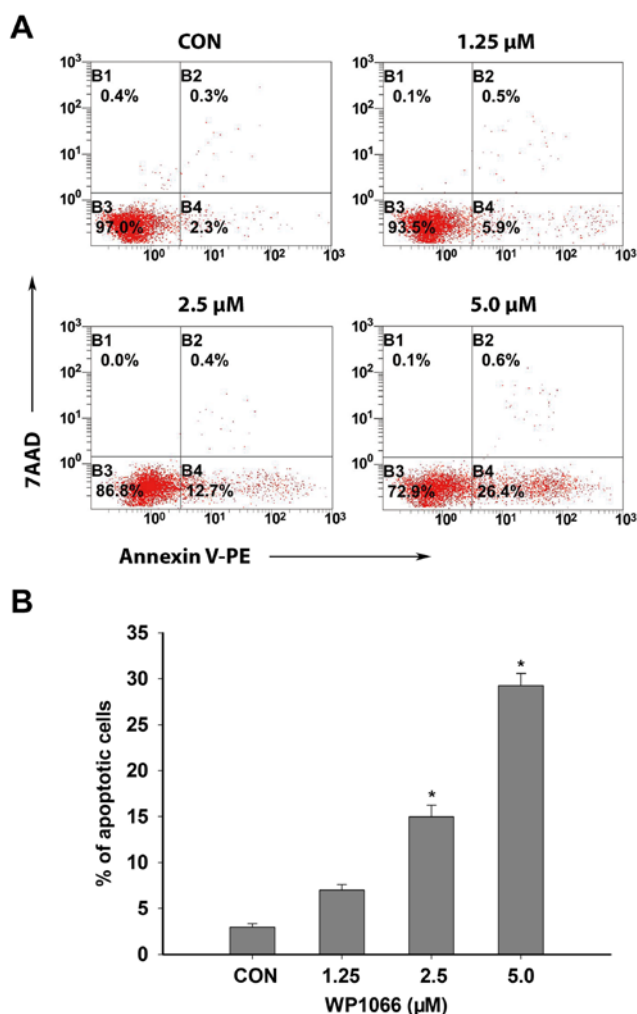


Figure 3. WP1066 induces apoptosis of SNK6 cells. (A) After exposure to WP1066 of different concentrations (1.25, 2.5 and 5.0  $\mu$ M) or 0.1% solvent (DMSO) for 24 h, apoptosis of SNK6 cells was quantified by Annexin V/7-aminoactinomycin D (7-AAD) flow cytometry. (B) The apoptosis ratio of SNK6 cells increased in a dose-dependent manner with the WP1066 treatment. Statistical data represent the mean  $\pm$  standard error of mean (SEM) of three independent experiments. \* $P$ <0.05, compared with control group.

in SNK6 cells (Fig. 1B). The inhibition of these pro-survival factors downstream of STAT3 pathway may be the potential mechanisms contributing to the antitumor effect of WP1066 in nasal NKTCL cells.

**Effect of WP1066 on mRNA levels of pro-survival genes related to STAT3 pathway in SNK6 cells.** To investigate the regulation of WP1066 on the oncogenic genes downstream of STAT3 pathway, the mRNA levels of c-Myc, cyclin D1, Bcl-2 genes were determined by RT-qPCR after WP1066 treatment with different concentrations for 24 h. The mRNA levels of these three genes were significantly downregulated after WP1066 treatment from moderate to high concentration in SNK6 cells (Fig. 4D).

## Discussion

STAT3 protein is known as an important effector of multiple growth factor receptors and cytokine signals to participate

in tumorigenesis by preventing apoptosis, enhancing proliferation, angiogenesis, invasiveness, chemoresistance, and immune evasion. Constitutive activation of the STAT3 pathway has been noted in a wide range of cancers and typically occurs in response to stimulation by tumor-promoting factors, including epidermal growth factor, IL-6, Tyr kinase, and many others (21,22). Inhibition of aberrantly activated STAT3 signaling pathway may present a novel antitumor strategy (Fig. 5). In our present study, constitutively protein expression of p-STAT3 was detected in both nasal NKTCL tissues and cell line (SNK6), suggesting the activation of STAT3 signal in this neoplasm. Moreover, immunohistochemical expression of p-STAT3 in nasal NKTCL tissues was found to be positively correlated with the Ki-67 levels in these cases with Fisher's exact test analysis. This was in accordance with previous studies of glioma and colorectal cancers in which STAT3 activation was generally correlated with poor prognosis (23,24).

Based on the published data, STAT3 has gained notoriety as a hub to relay multiple oncogenic signals modulating transcription of target genes. STAT3 was shown to promote growth and protect tumor cells against apoptosis by regulating genes encoding multiple oncogenic proteins, such as Bcl-2, Mcl-1, VEGF, c-Myc, and cyclin D1 (25-28). The evidence suggested that STAT3 was a promising candidate for antitumor target. WP1066 was a novel small molecule STAT3 inhibitor synthesized by modifying the structure of AG490 (a tyrosine kinase inhibitor to block JAK2 activity) (29,30). AG490 inhibited STAT3 only at high concentrations ( $IC_{50}$ , 50-100  $\mu$ M) and did not show significant antitumor effect in animal models (31,32). In contrast, WP1066 has exhibited significant antitumor activity against human cancer cells *in vitro* and in a xenograft mouse model, including gastric cancer, acute myelogenous leukaemia and melanoma (33-35).

Up to date, the exact working mechanism of WP1066 is largely unknown. This study evaluated the effect and mechanism of WP1066 in nasal NKTCL cells, and we demonstrated that WP1066 inhibited STAT3 activation and induced apoptosis in SNK6 nasal NKTCL cell line. Our findings indicated that the downregulation of c-Myc, cyclin D1, and Bcl-2 may partly contribute to the potential mechanisms for the antitumor effect of WP1066 in nasal NKTCL cells. The proliferation of SNK6 cells was significantly inhibited by WP1066 with  $IC_{50}$  concentration as  $2.62 \pm 0.28 \mu$ M at 24 h, which was similar to previous data described in renal cancer and erythroleukemia cell lines. Our results suggested that using WP1066 to inhibit the STAT3 signaling pathway could be a novel therapeutic strategy against nasal NKTCL.

To the best of our knowledge, our study is the first to report the antitumor effect and working mechanism of WP1066 through downregulation of p-STAT3 and downstream pro-survival molecules in nasal NKTCL. These findings showed that inhibitors of the STAT3 signaling pathway have enormous potential in the treatment of nasal NKTCL. Although crosstalk between STAT3 and other oncogenic signaling pathways deserve more exploration, this novel study contributes to further investigation on the useful biomarkers and potential therapeutic targets in nasal NKTCL. WP1066 is still undergoing preclinical and clinical trials which will provide novel insights into their antitumor activity, pharma-

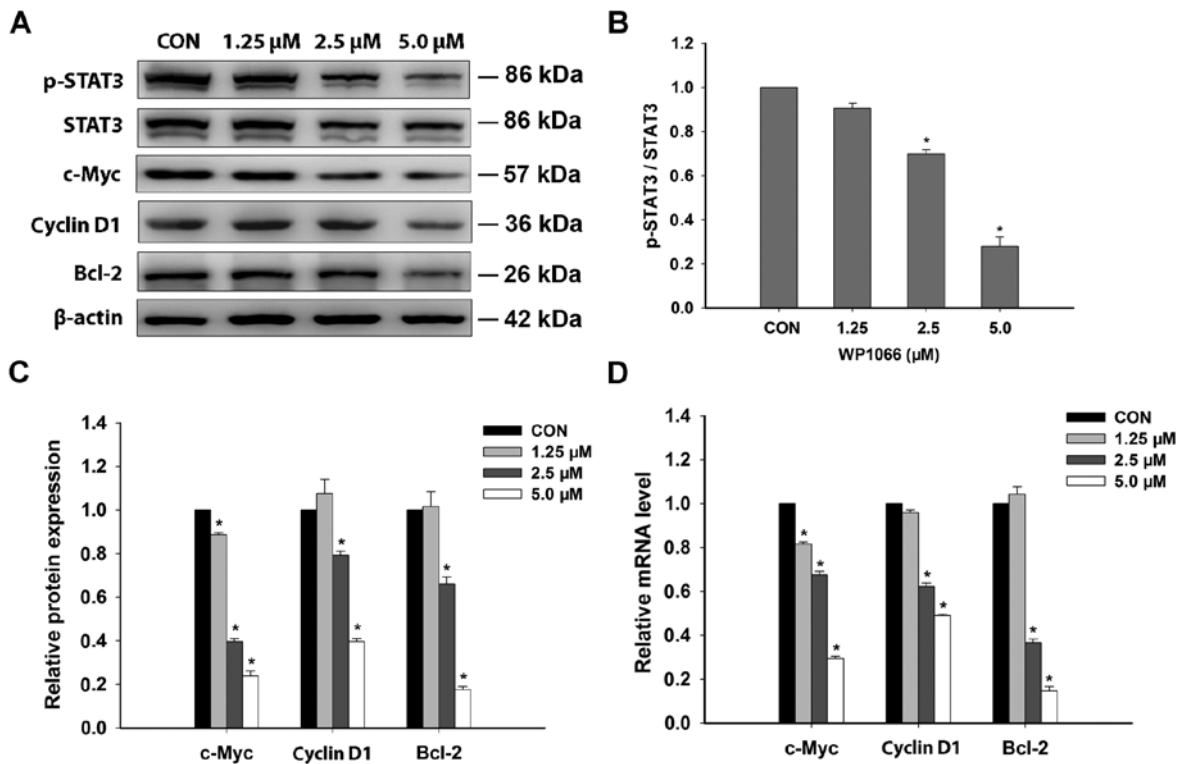


Figure 4. The influence of WP1066 on the protein and mRNA expression of potential pro-survival molecules in SNK6 cells. (A) Western blot analysis of WP1066 on protein expression of phospho-STAT3 (p-STAT3) and downstream molecules in SNK6 cells. (B) The inhibitory effect of WP1066 on phosphorylation of signal transducers and activators of transcription 3 (STAT3) in SNK6 cells after a 24-h treatment of WP1066 in a dose-dependent manner. (C) The significant reduction in the protein expression of c-Myc, cyclin D1, and Bcl-2 after WP1066 treatment from moderate to high concentration in SNK6 cells. (D) Effect of WP1066 on mRNA levels of c-Myc, cyclin D1, Bcl-2 in SNK6 cells. Statistical data represent the mean ± standard error of mean (SEM) of three independent experiments. \*P<0.05, compared with control group.

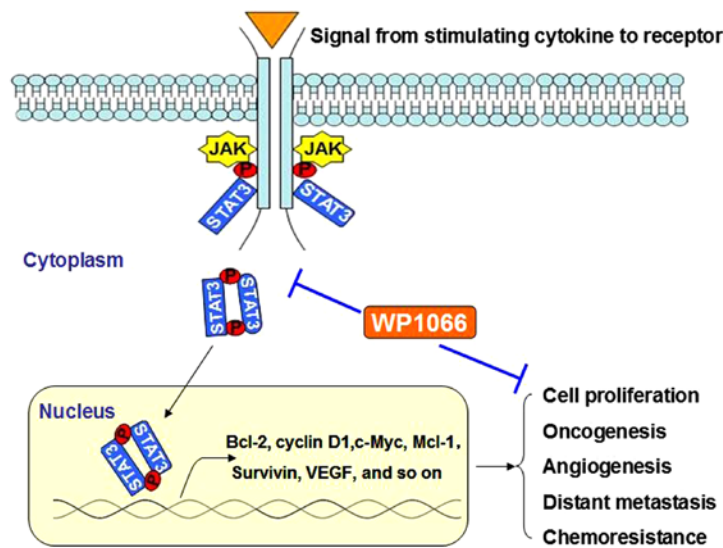


Figure 5. The signal transducers and activators of transcription 3 (STAT3) signaling pathway. Upon the activation of the STAT3 signaling by tumor-promoting factors, such as epidermal growth factor, interleukin (IL)-6, Tyr kinase, STAT3 were phosphorylated and dimerized. Activated STAT3 translocated into the nucleus and ultimately activated multiple downstream genes that facilitate tumor growth, invasion, metastasis, angiogenesis, and chemoresistance. WP1066 (a small molecular STAT3 inhibitor) represents a novel promising agent in antitumor therapy.

cokinetic, and toxicity (36). Moreover, the small molecule STAT3 inhibitor may be a promising combination for conventional chemotherapies to overcome or delay tolerance of nasal NK/TCL and improve the prognosis of this disease.

**Acknowledgements**

This study was partly supported by the National Natural Science Foundation (nos. 81473486 and 81270598), the National Public

HealthGrandResearchFoundation (no. 201202017), the Natural Science Foundation of Shandong Province (nos. ZR2012HZ003 and 2009ZRB14176), the Technology Development Projects of Shandong Province (nos. 2014GSF118021, 2010GSF10250 and 2008GG2NS02018), the Program of Shandong Medical Leading Talent, and the Taishan Scholar Foundation of Shandong Province.

## References

- Lima M: Aggressive mature natural killer cell neoplasms: From epidemiology to diagnosis. *Orphanet J Rare Dis* 8: 95, 2013.
- Roman E and Smith AG: Epidemiology of lymphomas. *Histopathology* 58: 4-14, 2011.
- Lim ST, Hee SW, Quek R, Lim LC, Yap SP, Loong EL, Sng I, Tan LH, Ang MK, Ngeow J, *et al*: Comparative analysis of extra-nodal NK/T-cell lymphoma and peripheral T-cell lymphoma: Significant differences in clinical characteristics and prognosis. *Eur J Haematol* 80: 55-60, 2008.
- Lee J, Park YH, Kim WS, Lee SS, Ryoo BY, Yang SH, Park KW, Kang JH, Park JO, Lee SH, *et al*: Extranodal nasal type NK/T-cell lymphoma: Elucidating clinical prognostic factors for risk-based stratification of therapy. *Eur J Cancer* 41: 1402-1408, 2005.
- Suzuki R: NK/T-cell lymphomas: Pathobiology, prognosis and treatment paradigm. *Curr Oncol Rep* 14: 395-402, 2012.
- Tse E and Kwong YL: Practical management of natural killer/T-cell lymphoma. *Curr Opin Oncol* 24: 480-486, 2012.
- Li H, Huang C, Huang K, Wu W, Jiang T, Cao J, Feng Z and Qiu Z: STAT3 knockdown reduces pancreatic cancer cell invasiveness and matrix metalloproteinase-7 expression in nude mice. *PLoS One* 6: e25941, 2011.
- Don-Doncow N, Escobar Z, Johansson M, Kjellström S, Garcia V, Munoz E, Sterner O, Bjartell A and Hellsten R: Galiellalactone is a direct inhibitor of the transcription factor STAT3 in prostate cancer cells. *J Biol Chem* 289: 15969-15978, 2014.
- Spaccarotella E, Pellegrino E, Ferracin M, Ferreri C, Cuccuru G, Liu C, Iqbal J, Cantarella D, Taulli R, Provero P, *et al*: STAT3-mediated activation of microRNA cluster 17~92 promotes proliferation and survival of ALK-positive anaplastic large cell lymphoma. *Haematologica* 99: 116-124, 2014.
- Koskela HL, Eldfors S, Ellonen P, van Adrichem AJ, Kuusanmäki H, Andersson EI, Lagström S, Clemente MJ, Olson T, Jalkanen SE, *et al*: Somatic STAT3 mutations in large granular lymphocytic leukemia. *N Engl J Med* 366: 1905-1913, 2012.
- Sansone P and Bromberg J: Targeting the interleukin-6/Jak/stat pathway in human malignancies. *J Clin Oncol* 30: 1005-1014, 2012.
- Jin HO, Lee YH, Park JA, Kim JH, Hong SE, Kim HA, Kim EK, Noh WC, Kim BH, Ye SK, *et al*: Blockage of Stat3 enhances the sensitivity of NSCLC cells to PI3K/mTOR inhibition. *Biochem Biophys Res Commun* 444: 502-508, 2014.
- Zhang C, Guo F, Xu G, Ma J and Shao F: STAT3 cooperates with Twist to mediate epithelial-mesenchymal transition in human hepatocellular carcinoma cells. *Oncol Rep* 33: 1872-1882, 2015.
- Yan CM, Zhao YL, Cai HY, Miao GY and Ma W: Blockage of PTPRJ promotes cell growth and resistance to 5-FU through activation of JAK1/STAT3 in the cervical carcinoma cell line C33A. *Oncol Rep* 33: 1737-1744, 2015.
- Munoz J, Dhillon N, Janku F, Watowich SS and Hong DS: STAT3 inhibitors: Finding a home in lymphoma and leukemia. *Oncologist* 19: 536-544, 2014.
- Oh MK, Park HJ, Kim NH, Park SJ, Park IY and Kim IS: Hypoxia-inducible factor-1 $\alpha$  enhances haptoglobin gene expression by improving binding of STAT3 to the promoter. *J Biol Chem* 286: 8857-8865, 2011.
- Chen L, Liu D, Zhang Y, Zhang H and Cheng H: The autophagy molecule Beclin 1 maintains persistent activity of NF- $\kappa$ B and Stat3 in HTLV-1-transformed T lymphocytes. *Biochem Biophys Res Commun* 465: 739-745, 2015.
- Liu ZQ, Han YC, Fang JM, Hu F, Zhang X and Xu Q: WITHDRAWN: Hypoxia-induced STAT3 contributes to chemoresistance and epithelial-mesenchymal transition in prostate cancer cells. *Biochem Biophys Res Commun* S0006-291X(15)00244-2, 2015.
- Horiguchi A, Asano T, Kuroda K, Sato A, Asakuma J, Ito K, Hayakawa M, Sumitomo M and Asano T: STAT3 inhibitor WP1066 as a novel therapeutic agent for renal cell carcinoma. *Br J Cancer* 102: 1592-1599, 2010.
- Lu K, Chen N, Zhou XX, Ge XL, Feng LL, Li PP, Li XY, Geng LY and Wang X: The STAT3 inhibitor WP1066 synergizes with vorinostat to induce apoptosis of mantle cell lymphoma cells. *Biochem Biophys Res Commun* 464: 292-298, 2015.
- Eiring AM, Page BD, Kraft IL, Mason CC, Vellore NA, Resatca D, Zabriskie MS, Zhang TY, Khorashad JS, Engar AJ, *et al*: Combined STAT3 and BCR-ABL1 inhibition induces synthetic lethality in therapy-resistant chronic myeloid leukemia. *Leukemia* 29: 586-597, 2015.
- Mills LD, Zhang Y, Marler RJ, Herreros-Villanueva M, Zhang L, Almada LL, Couch F, Wetmore C, Pasca di Magliano M and Fernandez-Zapico ME: Loss of the transcription factor GLI1 identifies a signaling network in the tumor microenvironment mediating KRAS oncogene-induced transformation. *J Biol Chem* 288: 11786-11794, 2013.
- Morikawa T, Baba Y, Yamauchi M, Kuchiba A, Nosho K, Shima K, Tanaka N, Huttenhower C, Frank DA, Fuchs CS, *et al*: STAT3 expression, molecular features, inflammation patterns, and prognosis in a database of 724 colorectal cancers. *Clin Cancer Res* 17: 1452-1462, 2011.
- Abou-Ghazal M, Yang DS, Qiao W, Reina-Ortiz C, Wei J, Kong LY, Fuller GN, Hiraoka N, Priebe W, Sawaya R, *et al*: The incidence, correlation with tumor-infiltrating inflammation, and prognosis of phosphorylated STAT3 expression in human gliomas. *Clin Cancer Res* 14: 8228-8235, 2008.
- de Groot J, Liang J, Kong LY, Wei J, Piao Y, Fuller G, Qiao W and Heimberger AB: Modulating antiangiogenic resistance by inhibiting the signal transducer and activator of transcription 3 pathway in glioblastoma. *Oncotarget* 3: 1036-1048, 2012.
- Kanterman J, Sade-Feldman M and Baniyash M: New insights into chronic inflammation-induced immunosuppression. *Semin Cancer Biol* 22: 307-318, 2012.
- Wang T, Yuan J, Zhang J, Tian R, Ji W, Zhou Y, Yang Y, Song W, Zhang F and Niu R: Anxa2 binds to STAT3 and promotes epithelial to mesenchymal transition in breast cancer cells. *Oncotarget* 6: 30975-30992, 2015.
- Yang C, He L, He P, Liu Y, Wang W, He Y, Du Y and Gao F: Increased drug resistance in breast cancer by tumor-associated macrophages through IL-10/STAT3/bcl-2 signaling pathway. *Med Oncol* 32: 352, 2015.
- Iwamaru A, Szymanski S, Iwado E, Aoki H, Yokoyama T, Fokt I, Hess K, Conrad C, Madden T, Sawaya R, *et al*: A novel inhibitor of the STAT3 pathway induces apoptosis in malignant glioma cells both in vitro and in vivo. *Oncogene* 26: 2435-2444, 2007.
- Hussain SF, Kong LY, Jordan J, Conrad C, Madden T, Fokt I, Priebe W and Heimberger AB: A novel small molecule inhibitor of signal transducers and activators of transcription 3 reverses immune tolerance in malignant glioma patients. *Cancer Res* 67: 9630-9636, 2007.
- Meydan N, Grunberger T, Dadi H, Shahar M, Arpaia E, Lapidot Z, Leeder JS, Freedman M, Cohen A, Gazit A, *et al*: Inhibition of acute lymphoblastic leukaemia by a Jak-2 inhibitor. *Nature* 379: 645-648, 1996.
- Horiguchi A, Oya M, Marumo K and Murai M: STAT3, but not ERKs, mediates the IL-6-induced proliferation of renal cancer cells. *ACHN and 769P. Kidney Int* 61: 926-938, 2002.
- Judd LM, Menhenniott TR, Ling H, Jackson CB, Howlett M, Kalantzis A, Priebe W and Giraud AS: Inhibition of the JAK2/STAT3 pathway reduces gastric cancer growth in vitro and in vivo. *PLoS One* 9: e95993, 2014.
- Ferrajoli A, Faderl S, Van Q, Koch P, Harris D, Liu Z, Hazan-Halevy I, Wang Y, Kantarjian HM, Priebe W, *et al*: WP1066 disrupts Janus kinase-2 and induces caspase-dependent apoptosis in acute myelogenous leukemia cells. *Cancer Res* 67: 11291-11299, 2007.
- Hatiboglu MA, Kong LY, Wei J, Wang Y, McEnery KA, Fuller GN, Qiao W, Davies MA, Priebe W and Heimberger AB: The tumor microenvironment expression of p-STAT3 influences the efficacy of cyclophosphamide with WP1066 in murine melanoma models. *Int J Cancer* 131: 8-17, 2012.
- Assi HH, Paran C, VanderVeen N, Savakus J, Doherty R, Petruzella E, Hoeschele JD, Appelman H, Raptis L, Mikkelsen T, *et al*: Preclinical characterization of signal transducer and activator of transcription 3 small molecule inhibitors for primary and metastatic brain cancer therapy. *J Pharmacol Exp Ther* 349: 458-469, 2014.